Sustainable Extraction and Processing of Raw Materials, 2026

# SUSTAINABLE MATERIALS FOR URANIUM REMOVAL FROM MINE WATER: COMPARATIVE EVALUATION OF ZERO-VALENT IRON NANOPARTICLES, CONVENTIONAL SORBENTS, AND FUNCTIONALISED MAGNETIC NANOMATERIALS

***Alexandre Loukanov[1,2]***

*[1]Laboratory of Engineering NanoBiotechnology, Department of Eng. Geoecology, University of Mining and Geology "St. Ivan Rilski", Sofia, Bulgaria, E-mail: a.loukanov@mgu.bg*
*[2]Department of Chemistry and Materials Science, National Institute of Technology, Gunma College, 580 Toriba, Maebashi, Gunma 371-8530 Japan, E-mail: loukanov@gunma-ct.ac.jp*

**ABSTRACT.** Uranium contamination of mine water and groundwater represents a significant environmental challenge associated with mining activities, ore processing, and radioactive waste management. In this study, uranium removal from aqueous solutions was comparatively evaluated using zero-valent iron nanoparticles (ZVINs), ligand-functionalised magnetic nanoparticles, water works sludge (WWS), and apatite under near-neutral conditions. The results revealed substantial differences in uranium immobilisation behaviour among the investigated materials. Water works sludge and apatite exhibited rapid uranium removal and reached near-equilibrium within a relatively short period, whereas ZVINs demonstrated slower but sustained uranium uptake over extended reaction times. This behaviour suggests that uranium immobilisation in $Fe^0$ systems is influenced by progressive nanoparticle aging and the formation of iron corrosion products. The observed trends are consistent with uranium immobilisation mechanisms previously reported for $Fe^0$-based systems, including adsorption onto iron oxides and hydroxides, co-precipitation with corrosion products, and possible reductive transformation of U(VI). In addition, amino-functionalised magnetic nanoparticles coated with a silsesquioxane polymer exhibited effective uranium adsorption and enabled rapid magnetic separation from aqueous solutions. Treatment of a 0.040 M uranium solution reduced the uranium concentration to approximately 0.014 M after 24 h, corresponding to about 64–65% removal efficiency, whereas uncoated magnetic nanoparticles exhibited negligible adsorption. Equilibrium adsorption data analysed using the Langmuir model indicated adsorption behaviour consistent with a finite number of active binding sites and confirmed the affinity of the amino-functionalised surface toward uranyl species within the investigated concentration range. The comparative results demonstrate that iron-based nanomaterials, particularly magnetically recoverable systems, may provide useful approaches for uranium removal and recovery from contaminated water. Although the experiments were conducted under simplified laboratory conditions, the findings provide a basis for further investigations in more complex mine-water systems, including the effects of competing ions, pH variability, sorbent regeneration, and long-term stability of immobilised uranium species.

**Key words:** uranium removal; zero-valent iron nanoparticles; magnetic nanoparticles; uranium immobilisation; mine water remediation; iron corrosion products.

## Introduction

The contamination of groundwater and mine water with uranium represents a significant environmental and public health concern associated with uranium mining, ore processing, radioactive waste disposal, and naturally occurring uranium-bearing geological formations (Loukanov et al., 2017; Abdessamed et al., 2023; Afrikaner et al., 2025). Soluble uranium species can migrate through aquatic systems and accumulate in groundwater resources, leading to long-term environmental risks and potential human exposure (Kairullova et al., 2026). Consequently, the development of efficient, economically viable, and environmentally sustainable methods for uranium removal and immobilisation remains a major challenge in environmental engineering and mine water remediation (Helal et al., 2025; Wu et al., 2026). Under oxidising conditions, uranium predominantly exists as hexavalent U(VI), typically forming soluble uranyl ions and carbonate complexes (Wazne et al., 2003). The mobility and persistence of uranium in groundwater are strongly influenced by pH, redox conditions, and the presence of competing ligands such as bicarbonate and phosphate ions (Skierszkan et al., 2021). Conventional treatment methods, including chemical precipitation, ion exchange, membrane filtration, coagulation, adsorption, and biological processes, are widely applied but often suffer from high operational costs, limited selectivity, formation of secondary waste, or insufficient long-term stability under complex environmental conditions (Akash et al., 2022; Lin et al., 2026). Iron-based materials have attracted increasing attention due to their low cost, high reactivity, and ability to immobilise inorganic contaminants and radionuclides (Zhao et al., 2020; Arahangelova et al., 2023; Fu et al., 2025; Loukanov et al., 2025). In particular, zero-valent iron nanoparticles (ZVINs) exhibit high specific surface area and strong reducing properties, enabling uranium removal through multiple mechanisms including adsorption onto iron corrosion products, reductive transformation of U(VI), and incorporation into iron oxide matrices (Riba et al., 2008; Sheng et al., 2014; Li et al., 2015; Gheju, 2025). During aqueous aging, $Fe^0$ nanoparticles undergo progressive transformation into ferrihydrite, FeOOH, maghemite and magnetite phases, which significantly influence uranium immobilisation behaviour (Wazne et al., 2003; Xiao et al., 2023; Gheju, 2025).

Although the fundamental mechanisms responsible for uranium removal by $Fe^0$-based systems are well established, several practical aspects relevant to environmental remediation remain insufficiently explored. In particular, comparatively limited attention has been devoted to the long-term evolution of uranium immobilisation during nanoparticle aging under near-neutral conditions representative of natural groundwater systems. Most previous studies have focused primarily on short-term removal efficiencies and mechanistic investigations, whereas the contribution of corrosion products generated during prolonged $Fe^0$ oxidation to sustained uranium stabilisation remains less clearly defined. Furthermore, direct comparisons between $Fe^0$ nanoparticles and alternative low-cost sorbents commonly considered for mine water treatment, such as apatite and water works sludge (WWS), are relatively scarce despite their practical relevance. Evaluations performed under comparable experimental conditions may therefore

provide useful information regarding the advantages and limitations of different uranium immobilisation strategies and their suitability for long-term environmental applications.

In parallel, magnetic nanomaterials functionalised with chelating ligands have emerged as promising candidates for uranium adsorption and recovery (Mahfouz et al., 2015). A key practical limitation of nanoscale adsorbents is their separation from treated water; magnetic nanoparticles address this challenge by enabling rapid recovery using an external magnetic field, thereby reducing the need for filtration and minimising secondary waste generation. Surface functionalisation with organosilane compounds introduces amino and chelating groups that enhance binding affinity toward uranyl ions while improving colloidal stability (Zhu et al., 2018). Such hybrid materials combine adsorption performance with magnetic recoverability and are increasingly investigated for environmental remediation applications (Ngerem et al., 2026).

While amino-functionalised magnetic adsorbents for uranium removal have been reported previously, studies integrating adsorption performance with practical considerations such as magnetic recovery, regeneration potential, and comparison with $Fe^0$-based immobilisation systems remain relatively limited. Consequently, further evaluation of these materials under conditions relevant to uranium-contaminated waters is warranted. In this context, the present study provides a comparative evaluation of uranium removal using zero-valent iron nanoparticles, apatite, and water works sludge under near-neutral conditions, with particular emphasis on the role of $Fe^0$ corrosion products in long-term uranium immobilisation. In addition, amino-functionalised magnetic nanoparticles coated with a silsesquioxane shell were investigated as magnetically recoverable adsorbents for uranium separation and recovery. Rather than proposing new uranium-removal mechanisms, the study aims to assess the relative performance, long-term behaviour, and practical advantages of different remediation approaches under comparable experimental conditions. Particular attention is given to sustained uranium stabilisation during $Fe^0$ aging and to the feasibility of combining adsorption with magnetic recovery. Comparative studies involving extended reaction times and multiple classes of remediation materials remain relatively limited in the literature, and the present work seeks to contribute to this area by providing a unified experimental evaluation under near-neutral aqueous conditions.

## Experimental procedures

### Synthesis of zero-valent iron nanoparticles

Zero-valent iron nanoparticles (ZVINs) were synthesised using a liquid-phase reduction method modified after the procedure reported by Sun et al. (2006), as shown on Figure 1A. Ferric chloride hexahydrate ($FeCl_3 \cdot 6H_2O$) was used as the iron precursor, while sodium borohydride ($NaBH_4$) served as the reducing agent. Briefly, 1.35 g of $FeCl_3 \cdot 6H_2O$ was dissolved in 50 mL of ultrapure Milli-Q water (18.2 MΩ·cm) under continuous magnetic stirring at ambient temperature. The pH of the precursor solution was adjusted to 6.8 using 4 M NaOH added dropwise in order to minimise premature hydrolysis and formation of ferric hydroxide species. Prior to reduction, the solution was purged with nitrogen to decrease dissolved oxygen concentration and minimise oxidation during nanoparticle synthesis. The reduction reaction was initiated by gradual addition of 2.0 g $NaBH_4$ dissolved in deoxygenated water under vigorous stirring. The immediate formation of black precipitates indicated the generation of nanoscale iron particles according to the following reaction:

$$2Fe^{3+} + 6BH_4^- + 18H_2O \rightarrow 2Fe^0 + 6B(OH)_3 + 21H_2$$

The reaction mixture was stirred for an additional 30 min to ensure complete reduction of ferric ions and homogeneous particle formation. The resulting nanoparticles were isolated by centrifugation at 6000 rpm and sequentially washed with deionised water, ethanol, and acetone (20 mL each) to remove residual salts, borates, and unreacted reagents. The purified nanoparticles were dried under reduced pressure (~$10^{-2}$ mbar) for 48 h and subsequently stored in an oxygen-free nitrogen glovebox (Saffron Scientific) prior to use in uranium adsorption experiments. Based on the synthesis route employed and previous reports describing borohydride-reduced nZVI materials (Sun et al., 2006), the synthesised material is expected to consist predominantly of nanoscale $Fe^0$ particles that may form chain-like aggregates as a consequence of magnetic dipole interactions. However, detailed structural characterisation of the synthesised nanoparticles was beyond the scope of the present study. Therefore, all discussion regarding nanoparticle morphology and surface structure is based on the established characteristics of similar nZVI materials reported in the literature.

### Surface functionalisation of magnetic nanoparticles with silsesquioxane polymer shell

Magnetically active iron oxide nanoparticles with an average particle size of 8–10 nm were functionalised using a silsesquioxane polymer shell containing ethylenediamine chelating groups capable of coordinating uranium ions and other heavy metals (Figure 1B). The synthesis strategy was designed to combine the magnetic separability of iron oxide nanoparticles with the selective adsorption properties of amine-containing organosilane ligands. Such hybrid nanomaterials have attracted increasing interest for environmental remediation applications due to their high surface area, tunable surface chemistry, and facile magnetic recovery from aqueous systems. The magnetic nanoparticles were coated through reaction with [N-(2-aminoethyl)-3-aminopropyl] trimethoxy-silane in toluene at 80 °C under continuous stirring. During the initial stage of the reaction, hydroxyl groups located on the nanoparticle surface reacted with methoxy groups of the silane molecules, resulting in formation of Fe–O–Si covalent bonds and methanol as a side product. Subsequent hydrolysis of residual alkoxy groups generated silanol functionalities that further condensed to produce an extended siloxane (Si–O–Si) network surrounding the magnetic nanoparticle core. Cross-linking reactions between adjacent silanol groups resulted in formation of a stable silsesquioxane polymer shell with a high density of accessible amino coordination sites. The overall coating process produced hybrid magnetic nanomaterials with improved colloidal stability and enhanced affinity toward uranyl ions through coordination interactions involving ethylenediamine functional groups. The polymer loading was estimated gravimetrically from the mass increase after the coating procedure and corresponded to approximately 22 wt.% relative to the initial nanoparticle mass. No additional spectroscopic or thermal analysis was performed to quantify the exact shell composition. Therefore, the proposed coating

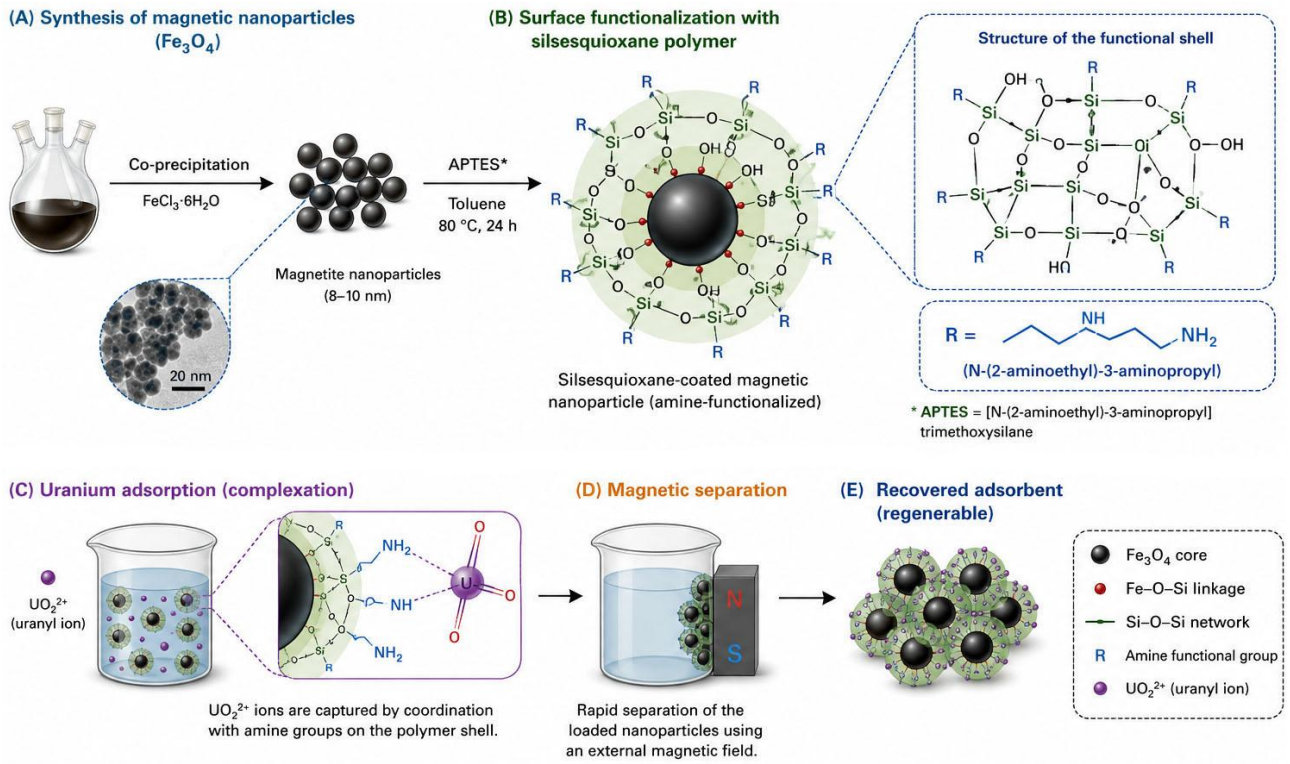



**Figure 1. Schematic representation of the preparation, surface functionalisation, uranium coordination, and magnetic separation process of silsesquioxane-coated magnetic nanoparticles**

structure should be regarded as a schematic representation based on the reaction chemistry of the silane precursor and literature reports describing similar silsesquioxane-coated magnetic nanoparticles. The resulting coating composition can be represented by the structural formula:

$$[(N-(2-aminoethyl)-3-aminopropyl)SiO_{1.5-x}(OH)_x]_n$$

The functionalised nanoparticles remained readily dispersible in aqueous media while preserving magnetic responsiveness, allowing rapid magnetic separation after uranium adsorption experiments. The presence of amino-functional groups is expected to promote uranium uptake through surface complexation and chelation mechanisms involving uranyl species (Figure 1C). The adsorption experiments reported in this study were conducted under near-neutral pH conditions (pH ≈ 7.2), and the observed adsorption behaviour should therefore be interpreted within this pH range only. Near-neutral pH was deliberately selected because one of the objectives of the study was to evaluate uranium removal and regeneration (Figure 1D,E) under environmentally relevant conditions that could potentially be applied without extensive chemical conditioning of contaminated waters. Such an approach is consistent with sustainable remediation strategies aimed at minimising reagent consumption and secondary waste generation. A systematic investigation of pH-dependent uranium speciation and adsorption behaviour was beyond the scope of the present work and should be addressed in future studies.

**Batch adsorption experiments**

Batch adsorption experiments were carried out to compare the uranium removal performance of zero-valent iron nanoparticles (ZVINs), apatite, water works sludge (WWS), and ligand-functionalised magnetic nanoparticles under near-neutral conditions. The apatite used in the experiments was laboratory-grade hydroxyapatite powder obtained from Sigma-Aldrich and used without additional purification. Water works sludge was collected from a local drinking water treatment facility following coagulation and sedimentation processes. Prior to use, the sludge was washed several times with deionised water, dried at 60 °C for 24 h, mechanically homogenised, and sieved to obtain particle sizes below 250 µm. Synthetic uranium-containing solutions were prepared by dissolving uranyl nitrate hexahydrate in deionised water. The initial uranium concentration for the batch experiments was adjusted to 20 mg/L unless otherwise stated. The experiments were intentionally performed using simplified synthetic uranium solutions to evaluate the intrinsic uranium removal performance of the investigated materials under controlled laboratory conditions.

The influence of competing ions commonly present in mine waters, including sulphate, carbonate, calcium, silica, and dissolved trace metals, was not investigated in the present study. Consequently, the reported results should be regarded as proof-of-concept laboratory data rather than a direct simulation of complex mine-water systems. The initial solution pH was adjusted to approximately 7.2 using diluted NaOH or $HNO_3$ solutions. Adsorption experiments were performed in 50 mL polypropylene centrifuge tubes containing 20 mL uranium solution and predetermined amounts of adsorbent material. The suspensions were continuously agitated using an orbital shaker operating at 150 rpm at room temperature (22 ± 2 °C). For kinetic experiments, independent replicate tubes were prepared for each sampling time in order to avoid changes in solution volume during the course of the experiment. At the designated contact time, the entire contents of a tube were centrifuged and the supernatant was collected for uranium analysis. In experiments involving magnetic nanoparticles, magnetic separation using an external permanent magnet was additionally applied. Residual uranium concentrations in the

supernatants were determined spectrophotometrically using the Arsenazo III method. Desorption and regeneration experiments were performed using uranium-loaded magnetic nanoparticles recovered after the adsorption step. Approximately 100 mg of the loaded adsorbent was contacted with 20 mL of 0.1 M $Na_2CO_3$ solution (solid-to-liquid ratio: 5 g/L) and agitated at 150 rpm for 2 h at room temperature (22 ± 2 °C). Following desorption, the nanoparticles were separated magnetically and the uranium concentration in the eluate was determined using the Arsenazo III method. Desorption efficiency was calculated as the percentage of previously adsorbed uranium released into the $Na_2CO_3$ solution. Regeneration experiments were conducted over three consecutive adsorption–desorption cycles under identical conditions. All experiments were conducted at least in duplicate, and the reported values represent average experimental results

## Results and discussions

### Time-dependent uranium removal by iron-based reactive materials

The uranium removal performance of water works sludge, apatite, and zero-valent iron nanoparticles (ZVINs) was evaluated under batch conditions at near-neutral pH. The time-dependent removal profiles are presented in Figure 2.

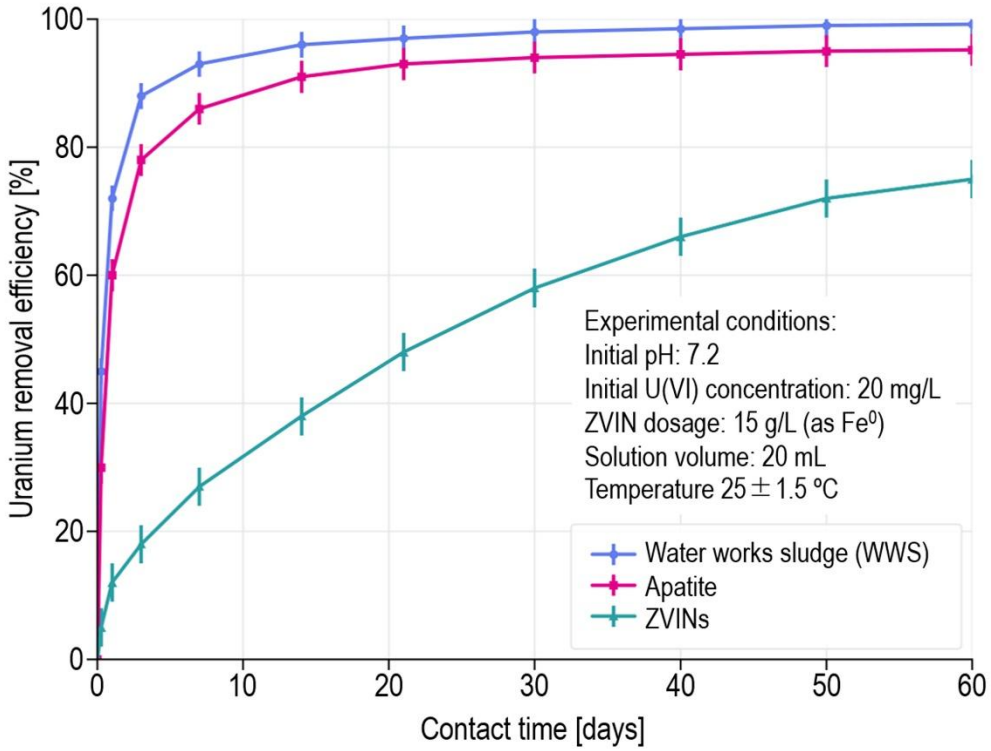



**Figure 2. Time-dependent uranium removal efficiency by water works sludge (WWS), apatatite, and zero-valent iton nanoparticles (ZVINs). Error bars represents standard deviation (n=3).**

The results demonstrated substantial differences in uranium immobilisation kinetics depending on the reactive material used. Adsorption onto WWS occurred rapidly during the initial contact period and reached near-equilibrium within approximately 72 h. Similar behaviour was observed for apatite, where uranium removal proceeded predominantly through adsorption and phosphate-assisted precipitation mechanisms.

In contrast, uranium removal by ZVINs proceeded more gradually and continued over extended reaction times exceeding 50 days. This behaviour indicates that uranium immobilisation by nanoscale iron systems is governed not only by initial surface adsorption but also by slower corrosion-mediated processes involving the progressive formation of iron hydroxides, oxides, and mixed Fe/U secondary phases. The gradual and continuously increasing uranium removal observed for ZVINs is consistent with previous studies reporting that nanoscale $Fe^0$ materials undergo dynamic surface evolution during aging in aqueous systems (Zhang et al., 2022). The progressive transformation of $Fe^0$ into ferrihydrite, FeOOH, maghemite, and magnetite phases generates additional reactive sites capable of uranium adsorption and co-precipitation. These differences in removal kinetics highlight that the mechanism of uranium immobilisation depends strongly on the physicochemical properties and reactivity of the material.

While WWS and apatite mainly act through relatively rapid adsorption and precipitation processes and reach near-equilibrium within a short time, ZVINs systems exhibit a slower but progressive removal trend without a clear equilibrium plateau within the investigated time frame. This observation suggests that surface transformation processes continue during nanoparticle aging, resulting in the gradual development of new reactive interfaces. Such prolonged reactivity may be advantageous for long-term groundwater remediation applications where sustained uranium immobilisation over extended periods is required, even if the overall removal efficiency remains lower than that achieved by WWS and apatite under the present experimental conditions. Recent investigations have demonstrated that uranium immobilisation by iron-based nanomaterials may involve several simultaneous mechanisms, including (Hua et al., 2023):

- surface complexation,
- reductive precipitation,
- incorporation into iron oxide lattices,
- adsorption onto corrosion products,
- and co-precipitation with secondary mineral phases.

The continuously increasing uranium removal observed for ZVINs over the 60-day experimental period therefore suggests that the progressive formation of iron corrosion products contributes to ongoing uranium immobilisation. Although the overall uranium removal efficiency remained lower than that obtained with WWS and apatite, the absence of a clear equilibrium plateau indicates that corrosion-mediated surface transformations continued throughout the experiment and may contribute to long-term uranium stabilisation. It should be noted that the present data do not directly identify the specific corrosion phases responsible for uranium fixation; therefore, the proposed interpretation should be regarded as consistent with the observed kinetic behaviour and previous mechanistic studies of Fe⁰-based remediation systems rather than as direct experimental proof (Anang et al., 2021).

**Mechanistic evidence for U(VI) co-precipitation with aging corrosion products**

The obtained results suggest that uranium immobilisation by ZVINs cannot be explained solely by direct interaction with metallic Fe⁰ surfaces. Instead, the data indicate that aging iron corrosion products likely play an important role in uranium fixation and long-term stabilisation. Based on the experimental conditions and approximate mass-balance considerations, a limited fraction of the initial Fe⁰ was assumed to undergo oxidation during the investigated reaction period. No direct phase-specific quantification of Fe⁰ oxidation products was performed in the present study. The partial oxidation of Fe⁰ resulted in the formation of substantial quantities of amorphous and poorly crystalline iron oxides and hydroxides. These secondary phases are known to possess strong affinity toward uranyl species and may act as efficient scavengers for dissolved uranium. Based on the experimental conditions and estimated extent of Fe⁰ oxidation, the Fe molar ratio associated with the resulting corrosion products was approximately 154 (Table 1).

Table 1. *Experimental conditions and estimated Fe : U molar ratio in corrosion products formed during uranium immobilisation experiments*

| Initial pH | $Fe^0$ dosage mg/L | Initial U(VI) concn., mg/L | Solution volume, mL | Estimated Fe:U ratio |
|---|---|---|---|---|
| 7.2 | 15 | 20 | 20 | 154 |

Such a high Fe ratio indicates that uranium represents only a minor component incorporated within a large excess of iron corrosion phases. Consequently, direct detection of uranium-bearing crystalline phases by conventional X-ray diffraction would be expected to be difficult. The obtained results are consistent with previous report indicating that uranium immobilisation in iron-based systems frequently occurs through mixed adsorption/co-precipitation pathways rather than through purely reductive precipitation mechanisms (Kong et al., 2016). In particular, the progressive transformation of Fe⁰ into magnetite and FeOOH phases may generate highly reactive surfaces capable of retaining uranyl ions through several pathways, including:

- incorporation within into magnetite lattices,
- formation of U–O–Fe surface complexes,
- and entrapment within amorphous iron hydroxide matrices.

The persistence of immobilised uranium in the ZVINs system, together with the continuously increasing removal observed during long-term aging, is consistent with the possibility of partial structural incorporation and co-precipitation within iron corrosion products rather than weak reversible adsorption alone (Figure 3). Visual observations during the experiments also indicated gradual darkening and aggregation of the nanoparticles, suggesting progressive surface oxidation and formation of mixed Fe(II)/Fe(III) phases.

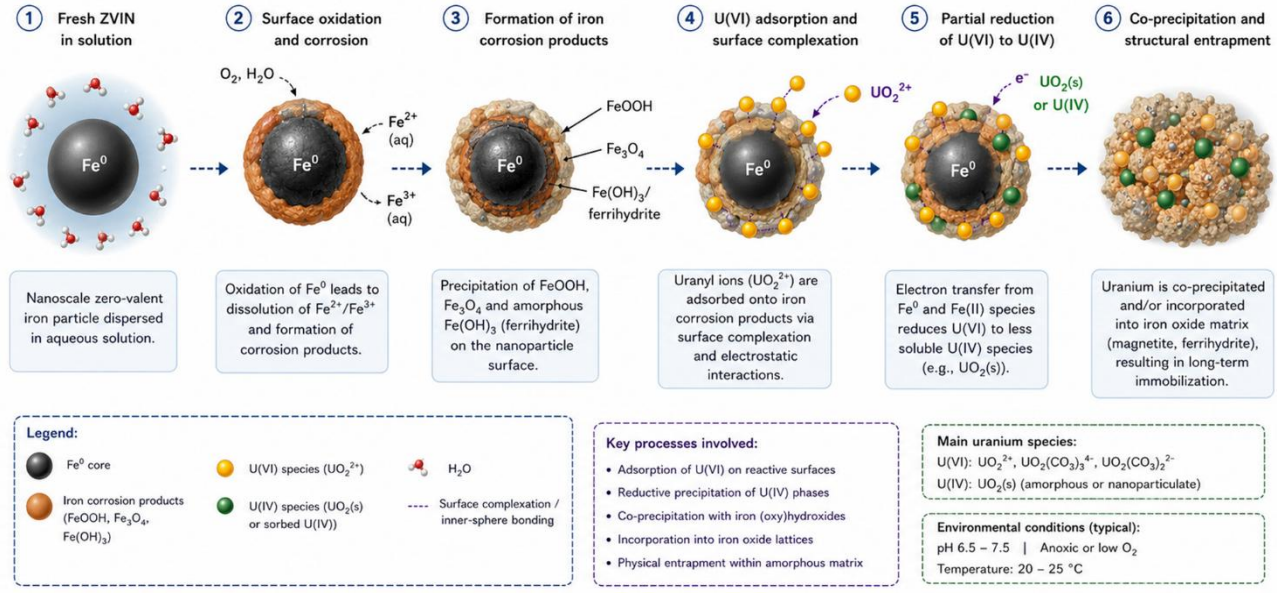



**Figure 3. Schematic illustration of the proposed mechanisms responsible for uranium immobilisation by zero-valent iron nanoparticles. Multiple processes including adsorption, reduction, co-precipitation and structural incorporation contribute to the long term stabilisation of uranium**

The proposed mechanism therefore suggests that uranium stabilisation is governed by coupled adsorption-corrosion processes rather than by direct reduction alone. Progressive oxidation of $Fe^0$ nanoparticles generates reactive iron oxide and hydroxide phases that provide additional adsorption and co-precipitation sites for dissolved uranium species. Simultaneously, electron transfer from $Fe^0$ and Fe(II)-containing corrosion products may promote partial reduction of soluble U(VI) species to less mobile forms. The combined action of surface complexation, co-precipitation, reductive transformation, and structural incorporation within aging iron corrosion matrices is therefore likely responsible for the long-term immobilisation and decreased mobility of uranium under the investigated experimental conditions. The inability to desorb a significant fraction of immobilised uranium using $Na_2CO_3$ further supports the hypothesis of partial structural incorporation rather than weak reversible adsorption. Moreover, visual observations during the experiments indicated gradual darkening and aggregation of the nanoparticles, suggesting progressive surface oxidation and formation of mixed Fe(II)/Fe(III) phases. Such transformations are widely recognized as critical factors controlling uranium stabilisation in iron-based remediation systems (Roberts et al., 2017).

**Uranium separation by ligand-functionalised magnetic nanoparticles**

The uranium adsorption properties of silsesquioxane-coated magnetic nanoparticles were investigated using aqueous uranyl nitrate solutions followed by magnetic separation. Treatment of 10 mL of a 0.040 M uranyl nitrate solution with 0.1 g of functionalised magnetic nanoparticles for 24 h resulted in a decrease in uranium concentration from 0.040 M to 0.0145 M, corresponding to approximately 64% uranium removal efficiency under the investigated conditions. In contrast, uncoated magnetic nanoparticles exhibited negligible uranium uptake, indicating that the ethylenediamine-functionalised silsesquioxane shell plays a dominant role in uranium coordination and adsorption. The enhanced adsorption performance can be attributed to the presence of amino donor groups capable of forming coordination complexes with uranyl ions according to the following interaction scheme:

$$Fe_3O_4{-}Si{-}(NH_2)_2 + UO_2^{2+} \rightarrow Fe_3O_4{-}Si{-}(NH_2)_2{\cdot}UO_2^{2+}$$

The magnetic properties of the developed nanomaterial enabled rapid separation of the uranium-loaded adsorbent from aqueous suspension within several minutes after application of an external magnetic field. This represents a significant practical advantage for the treatment of contaminated mine water, where separation of nanoscale adsorbents is often technically challenging.

**Adsorption Isotherm study**

To evaluate adsorption performance over a broader concentration range, equilibrium adsorption experiments were conducted using initial uranium concentrations between 0.005 and 0.150 M while maintaining a constant adsorbent dosage (0.1 g) and contact time (24 h). The obtained results are summarised in Table 2. The expanded dataset comprises nine equilibrium concentration points spanning more than one order of magnitude, providing a substantially improved basis for evaluation of equilibrium adsorption behaviour and isotherm analysis compared with the original dataset. The results demonstrate that the amino-functionalised silsesquioxane coating provides substantial uranium uptake under all investigated conditions. At lower uranium concentrations, removal efficiencies reached approximately 68–70%, indicating strong affinity of the chelating amino groups toward dissolved uranyl species. As the initial uranium concentration increased, the removal efficiency gradually decreased to approximately 37%, reflecting progressive occupation of available adsorption sites and the approach toward sorbent saturation. Despite this trend, significant uranium removal was maintained even at elevated concentrations, confirming the strong adsorption capability of the functionalised magnetic nanomaterial. The observed concentration-dependent behaviour is consistent with adsorption processes involving a finite number of energetically favourable binding sites.

Table 2. *Equilibrium adsorption data for uranium uptake by ligand-functionalised magnetic nanoparticles used for Langmuir isotherm analysis*

| Initial U concn. (M) | Adsorbent dosage (g) | Contact time (h) | Final U concentration (M) | Removal efficiency (%) |
|---|---|---|---|---|
| 0.005 | 0.1 | 24 | 0.0015 | 70 |
| 0.01 | 0.1 | 24 | 0.0032 | 68 |
| 0.02 | 0.1 | 24 | 0.0076 | 62 |
| 0.04 | 0.1 | 24 | 0.0145 | 64 |
| 0.05 | 0.1 | 24 | 0.018 | 64 |
| 0.06 | 0.1 | 24 | 0.0235 | 61 |
| 0.08 | 0.1 | 24 | 0.034 | 58 |
| 0.1 | 0.1 | 24 | 0.052 | 48 |
| 0.15 | 0.1 | 24 | 0.095 | 37 |

**Langmuir isotherm analysis**

The equilibrium adsorption data were analysed using the Langmuir adsorption model:

$$q_e = (q_{max}\, K_L C_e) / (1 + K_L\, C_e)$$

where $q_e$ (mmol/g) is the equilibrium adsorption capacity, $q_{max}$ (mmol/g) is the maximum monolayer adsorption capacity, $K_L$ (L/mol) is the Langmuir affinity constant, $C_e$ (mol/L) is the equilibrium uranium concentration in solution. The corresponding Langmuir isotherm is presented in Figure 4.

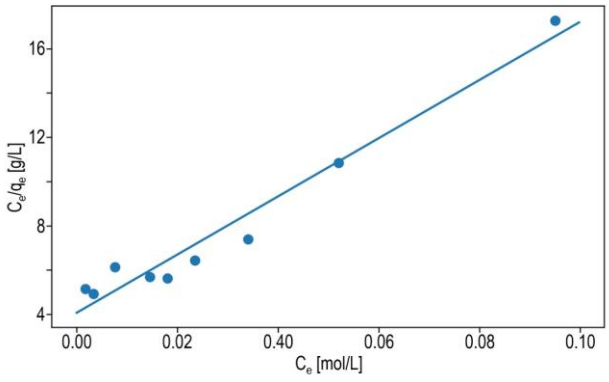



**Figure 4. Langmuir isotherm for uranium adsorption onto ligand-functionalised magnetic nanoparticles**

Linear regression analysis of the linearised Langmuir equation yielded a coefficient of determination ($R^2$) of 0.97, indicating satisfactory agreement between the experimental data and the Langmuir adsorption model. The estimated maximum adsorption capacity was approximately 5.8 mmol U/g. Although the investigated concentration range does not span multiple orders of magnitude, the expanded dataset provides a reasonable basis for preliminary Langmuir analysis and evaluation of adsorption performance. Therefore, the Langmuir model is used here as an empirical approximation of the adsorption behaviour rather than a definitive mechanistic description. The observed adsorption behaviour is consistent with coordination interactions between uranyl ions and amino-functional groups incorporated within the silsesquioxane coating. Nevertheless, additional factors such as surface heterogeneity, multilayer adsorption, or partial precipitation may also contribute to uranium uptake under certain conditions. The Langmuir model was selected as an initial approximation of the adsorption process. Evaluation of additional adsorption models such as Freundlich and Temkin could provide further mechanistic insight and will be considered in future investigations. Despite these limitations, the isotherm analysis confirms the substantial adsorption affinity of the functionalised magnetic nanomaterial toward uranium species. In combination with the rapid magnetic separation capability of the material, these results indicate that amino-functionalised magnetic nanoparticles represent promising candidates for uranium recovery and remediation applications in contaminated aqueous systems.

**Desorption and regeneration**

To further evaluate the regeneration potential of the developed nanomaterials, desorption experiments were performed using $Na_2CO_3$ solution as an eluent. Approximately 48 ± 5% of the adsorbed uranium was desorbed under the investigated conditions, indicating partial reversibility of the adsorption process (Table 3).

Table 3. *Regeneration cycles (magnetic nanoparticles)*

| Cycle | Removal efficiency, % | Desorption efficiency, % |
|---|---|---|
| 1 | 65 ± 2 | 48 ± 5 |
| 2 | 60 ± 3 | 45 ± 4 |
| 3 | 55 ± 3 | 42 ± 4 |

These results demonstrate that a substantial fraction of the adsorbed uranium can be recovered, while another fraction remains strongly immobilised on the adsorbent surface. The regeneration experiments should be considered preliminary and were included primarily to assess the feasibility of adsorbent reuse rather than to provide a comprehensive optimisation of regeneration conditions. The incomplete desorption suggests that a significant fraction of uranium is strongly bound to the nanoparticle surface or retained through more stable immobilisation mechanisms. Regeneration tests over three consecutive adsorption-desorption cycles showed that the removal efficiency decreased gradually from 65% to 55%, while desorption efficiency decreased from approximately 48% to 42%. These results indicate that the magnetic nanoparticles exhibit moderate regeneration capability, although partial loss of adsorption performance occurs during repeated use. This behaviour is consistent with a combination of reversible surface adsorption and stronger uranium immobilisation mechanisms.

An important practical advantage of the developed material is the possibility of rapid magnetic separation after adsorption, which simplifies recovery of the adsorbent from treated water and may reduce the need for additional solid-liquid separation processes. Together with the moderate regeneration capability demonstrated in the present study, this characteristic may facilitate repeated use of the adsorbent and improve process sustainability. Although the present study was conducted under controlled laboratory conditions using synthetic uranium solutions, the obtained results demonstrate that amino-functionalised magnetic nanoparticles possess substantial uranium adsorption capacity and can be readily recovered using an external magnetic field. Further investigations should focus on optimisation of regeneration efficiency, evaluation of adsorption performance in the presence of competing ions, and assessment of long-term material stability under environmentally relevant conditions. Nevertheless, the results indicate that functionalised magnetic nanomaterials represent promising candidates for uranium remediation technologies combining selective adsorption and magnetic recovery.

## Conclusion

This study demonstrates that iron-based nanomaterials provide effective approaches for uranium removal and immobilisation under near-neutral aqueous conditions. Zero-valent iron nanoparticles (ZVINs) exhibited gradual but sustained uranium removal over extended reaction times, in contrast to the rapid but equilibrium-limited behaviour observed for water works sludge and apatite. The time-dependent removal profile suggests that uranium immobilisation in $Fe^0$ systems is governed by coupled adsorption and corrosion processes, with progressive formation of iron corrosion products likely contributing to continued uranium uptake. The experimental results are consistent with uranium immobilisation mechanisms reported in the literature for $Fe^0$-based systems, including surface complexation, co-precipitation, reductive transformation, and incorporation into aging iron corrosion products. Although these mechanisms were not directly resolved at the phase level, the observed kinetic behaviour and limited desorption support the role of corrosion products in long-term uranium stabilisation. Ligand-functionalised magnetic nanoparticles demonstrated substantial uranium adsorption capacity and enabled rapid magnetic separation from aqueous solutions. The adsorption behaviour is consistent with coordination interactions between uranyl ions and amino-functional groups, while regeneration experiments indicate moderate reusability with partial irreversible binding of uranium. These characteristics highlight the potential of such materials for applications where both adsorption efficiency and facile recovery are required. Overall, the results suggest that functionalising magnetically recoverable iron nanoparticles offers a versatile approach for uranium remediation. However, the present study was conducted under controlled laboratory conditions using simplified aqueous systems, and further investigations are required to evaluate performance in complex mine-water matrices, including the effects of competing ions, pH variability, and long-term stability. Future work should focus on detailed characterisation of corrosion products, validation under realistic

mine-water conditions, and optimisation of adsorption and regeneration processes.

## References


Abdessamed, D., Jodar-Abellan, A., Ghoneim, S. S. M., Almaliki, A., Hussein, E. E., & Pardo, M. Á. (2023). Groundwater quality assessment for sustainable human consumption in arid areas based on GIS and water quality index in the watershed of Ain Sefra (SW of Algeria). *Environmental Earth Sciences, 82*(21), Article 510. https://doi.org/10.1007/s12665-023-11183-9

Afrikaner, L. C., Mapani, B., & Amwele, H. (2025). Groundwater in arid environments: A review of uranium occurrence and impacts. Journal of Hydrology*: Regional Studies, 62*, Article 102814. https://doi.org/10.1016/j.ejrh.2025.102814

Akash, S., Sivaprakash, B., Vadivel Raja, V. C., Rajamohan, N., & Muthusamy, G. (2022). Remediation techniques for uranium removal from polluted environment – Review on methods, mechanism and toxicology. *Environmental Pollution, 302*, Article 119068. https://doi.org/10.1016/j.envpol.2022.119068

Anang, E., Hong, L., Fan, X., & Asamoah, E. N. (2022). Attapulgite supported nanoscale zero-valent iron in wastewater treatment and groundwater remediation: synthesis, application, performance and limitation. *Environmental Technology Reviews, 11,* 1-17. https://doi.org/10.1080/21622515.2021.2010131

Arahangelova, V., & Loukanov, A. (2023). Phytoremediation and extraction of colloidal contaminants from mine effluents through legume plants. *Sustainable Extraction and Processing of Raw Materials Journal (SEPRM), 4,* 6–10. https://doi.org/10.58903/u17190823

Fu, W., Liu, Z., Yang, Z., Li, Y., & Pan, B. (2025). Confined iron-based nanomaterials for water decontamination: Fundamentals, applications, and challenges. *Fundamental Research, 5*(2), 612–623. https://doi.org/10.1016/j.fmre.2023.07.011

Gheju, M. (2025). Mechanisms of contaminant removal with metallic iron (Fe0): A comprehensive and critical review. *Separation and Purification Technology, 364*(Part 3), Article 132503. https://doi.org/10.1016/j.seppur.2025.132503

Helal, A. S., Hémadi, M., Lomas, J. S., Ammar, S., Abdelhafiz, A., El-Sheikh, S. M., Sheta, S. M., Galanek, M., Hassan, M. H., Chang, J.-K., & Li, J. (2025). Uranium removal from environmental water and nuclear waste: Nanomaterial solutions and their environmental sustainability. *Chemical Engineering Journal, 507,* Article 160298. https://doi.org/10.1016/j.cej.2025.160298

Hua, Y., Li, D., Zou, J., Wang, W., Wu, X., Zhang, X., Liu, Q., Zhao, G., Li, M., Zhang, W-x., & Yang, J. (2023). Evolutional solid phase and solid-liquid interface uranium immobilisation mechanisms by nanoscale zero-valent iron and enhanced uranium stability control strategy. *Chemical Engineering Journal, 453,* 139924. 10.1016/j.cej.2022.139924

Kairullova, M., Bakhtin, M., Ilbekova, K., & Ibrayeva, D. (2026). Migration and accumulation of uranium-associated heavy metals in mining-affected ecosystems (water, soil, and plants). *Biology, 15*(6), Article 502. https://doi.org/10.3390/biology15060502

Kong, L., Zhu, Y., Wang, M., Li, Z., Tan, Z., Xu, R., Tang, H., Chang, X., Xiong, Y., & Chen, D. (2016). Simultaneous reduction and adsorption for immobilisation of uranium from aqueous solution by nano-flake Fe-SC. *Journal of Hazardous Materials, 320,* 435–441. doi: 10.1016/j.jhazmat.2016.08.060

Li, Z.-J., Wang, L., Yuan, L.-Y., Xiao, C.-L., Mei, L., Zheng, L.-R., Zhang, J., et al. (2015). Efficient removal of uranium from aqueous solution by zero-valent iron nanoparticle and its graphene composite. *Journal of Hazardous Materials, 290*, 26–33. https://doi.org/10.1016/j.jhazmat.2015.02.028

Lin, K., Wan, Y., Chang, H., Yu, H., Yang, H., & Qu, F. (2026). Advances and challenges in remediation technologies for uranium/radium-contaminated groundwater. *Environmental Science: Water Research & Technology, 12*, 769–788. https://doi.org/10.1039/D5EW00910C

Loukanov, A. (2025). Magnetic nanoparticle-assisted remediation of petroleum-contaminated soils. Sustainable Extraction and Processing of Raw Materials Journal (SEPRM), 6, 51–59. https://doi.org/10.58903/dw18922073

Loukanov, A., Udono, H., Takakura, R., Mladenova, P., Kobayashi, N., Kawamura, R., & Nakabayashi, S. (2017). Monitoring and extraction of uranium in polluted acid mine drainage by super-paramagnetic nanoparticles coated with carbon nanodots. *Journal of Radioanalytical and Nuclear Chemistry, 314*, 1149–1159. https://doi.org/10.1007/s10967-017-5471-z

Mahfouz, M. G., Galhoum, A. A., Gomaa, N. A., Abdel-Rehem, S. S., Atia, A. A., Vincent, T., & Guibal, E. (2015). Uranium extraction using magnetic nano-based particles of diethylenetriamine-functionalised chitosan: Equilibrium and kinetic studies. *Chemical Engineering Journal, 262,* 198–209. https://doi.org/10.1016/j.cej.2014.09.061

Ngerem, E. C., Sanusi, I. A., Dalu, T., & Suinyuy, T. N. (2026). Sustainable acid mine drainage wastewater remediation: A comprehensive review and bibliometric analysis. *Environmental Science Advances, 5*(3), 681–710. https://doi.org/10.1039/d5va00266d

Riba, O., Scott, T. B., Ragnarsdottir, K. V., & Allen, G. C. (2008). Reaction mechanism of uranyl in the presence of zero-valent iron nanoparticles. *Geochimica et Cosmochimica Acta, 72*(16), 4047–4057. https://doi.org/10.1016/j.gca.2008.04.041

Roberts, H., Morris, K., Law, G., Mosselmans, J., Bots, P., Kvashnina, K., & Shaw, S. (2017). Uranium(V) Incorporation Mechanisms and Stability in Fe(II)/Fe(III) (oxyhydr)Oxides. *Environmental Science & Technology Letters, 4,* 421–426. https://doi.org/10.1021/acs.estlett.7b00348

Sheng, G., Shao, X., Li, Y., Li, J., Dong, H., Cheng, W., Gao, X., & Huang, Y. (2014). Enhanced removal of uranium(VI) by nanoscale zerovalent iron supported on Na–bentonite and an investigation of mechanism. *Journal of Physical Chemistry A, 118*(16), 2952–2958. https://doi.org/10.1021/jp412404w

Skierszkan, E. K., Dockrey, J. W., Helsen, J., Findlater, L.-L., Bataille, C. P., de Laplante, G., McBeth, J. M., Mayer, K. U., & Beckie, R. D. (2021). Persistence of uranium in old

and cold subpermafrost groundwater indicated by linking 234U-235U-238U, groundwater ages, and hydrogeochemistry. *ACS Earth and Space Chemistry, 5*(12), 3474–3487. https://doi.org/10.1021/acsearthspacechem.1c00307

Sun, Y.-P., Li, X.-Q., Cao, J., Zhang, W.-X., & Wang, H. P. (2006). Characterization of zero-valent iron nanoparticles. *Advances in Colloid and Interface Science, 120*(1–3), 47–56. https://doi.org/10.1016/j.cis.2006.03.001

Verma, Y., Verma, A., Bhaskaralingam, A., Dhiman, P., Wang, T., Kumar, A., & Sharma, G. (2025). Application of zero-valent iron and its derivatives in the removal of toxic metal ions from groundwater. *Water, 17*(10), Article 1524. https://doi.org/10.3390/w17101524

Wazne, M., Korfiatis, G. P., & Meng, X. (2003). Carbonate effects on hexavalent uranium adsorption by iron oxyhydroxide. *Environmental Science & Technology, 37*(16), 3619–3624. https://doi.org/10.1021/es034166m

Wu, R., Wang, X., He, S., Wu, M., Li, P., Show, P.-L., Han, P., Hamzah, M. H., Zhang, Y., & Chen, J. (2026). Robust immobilisation of uranium using biogenic FeS with lignocellulose from green plant waste. *Chemical Engineering Journal, 528*, Article 172352. https://doi.org/10.1016/j.cej.2025.172352

Xiao, Y., Helal, A. S., Mozario, E., Mayoral, A. et al. (2023). Functionalized maghemite nanoparticles for enhanced adsorption of uranium from simulated wastewater and magnetic harvesting. *Environmental Research, 216*(2), 114569. https://doi.org/10.1016/j.envres.2022.114569

Zhang, X., Liu, X., Peng, Y., Wu, X., Tan, Y., Zeng, Q., Song, Z. & Li, M. (2022). Controllable shell corrosion of coated nanoscale zero valent iron induces long-term potentiation of its reactivity for uranium removal. *Separation and Purification Technology, 287,* 120550. https://doi.org/10.1016/j.seppur.2022.120550

Zhao, X., Liu, W., Cai, Z., Fu, J., Duan, J., Zhao, D., Bozack, M.& Feng, Y. (2020). Reductive immobilisation of uranium by stabilised zero-valent iron nanoparticles: Effects of stabilisers, water chemistry and long-term stability. *Colloids and Surfaces A: Physicochemical and Engineering Aspects, 604,* 125315. 10.1016/j.colsurfa.2020.125315

Zhu, N., Ji, H., Yu, P., Niu, J., Farooq, M. U., Akram, M. W., Udego, I. O., Li, H., & Niu, X. (2018). Surface modification of magnetic iron oxide nanoparticles. *Nanomaterials, 8(*10), Article 810. https://doi.org/10.3390/nano8100810)